Surface ocean iron fertilization: The role of airborne volcanic ash from subduction zone and hot spot volcanoes and related iron fluxes into the Pacific Ocean

Nazlı Olgun,[1,2] Svend Duggen,[1,3] Peter Leslie Croot,[2,4] Pierre Delmelle,[5] Heiner Dietze,[2] Ulrike Schacht,[6] Niels Óskarsson,[7] Claus Siebe,[8] Andreas Auer,[9] and Dieter Garbe-Schönberg[10]

Received 15 December 2009; revised 15 March 2011; accepted 8 June 2011; published 1 October 2011.

[1] Surface ocean iron (Fe) fertilization can affect the marine primary productivity (MPP), thereby impacting on CO_2 exchanges at the atmosphere-ocean interface and eventually on climate. Mineral (aeolian or desert) dust is known to be a major atmospheric source for the surface ocean biogeochemical iron cycle, but the significance of volcanic ash is poorly constrained. We present the results of geochemical experiments aimed at determining the rapid release of Fe upon contact of pristine volcanic ash with seawater, mimicking their dry deposition into the surface ocean. Our data show that volcanic ash from both subduction zone and hot spot volcanoes (n = 44 samples) rapidly mobilized significant amounts of soluble Fe into seawater (35–340 nmol/g ash), with a suggested global mean of 200 ± 50 nmol Fe/g ash. These values are comparable to the range for desert dust in experiments at seawater pH (10–125 nmol Fe/g dust) presented in the literature (Guieu et al., 1996; Spokes et al., 1996). Combining our new Fe release data with the calculated ash flux from a selected major eruption into the ocean as a case study demonstrates that single volcanic eruptions have the potential to significantly increase the surface ocean Fe concentration within an ash fallout area. We also constrain the long-term (millennial-scale) airborne volcanic ash and mineral dust Fe flux into the Pacific Ocean by merging the Fe release data with geological flux estimates. These show that the input of volcanic ash into the Pacific Ocean (128–221 × 10^{15} g/ka) is within the same order of magnitude as the mineral dust input (39–519 × 10^{15} g/ka) (Mahowald et al., 2005). From the similarity in both Fe release and particle flux follows that the flux of soluble Fe related to the dry deposition of volcanic ash (3–75 × 10^9 mol/ka) is comparable to that of mineral dust (1–65 × 10^9 mol/ka). Our study therefore suggests that airborne volcanic ash is an important but hitherto underestimated atmospheric source for the Pacific surface ocean biogeochemical iron cycle.

Citation: Olgun, N., S. Duggen, P. L. Croot, P. Delmelle, H. Dietze, U. Schacht, N. Óskarsson, C. Siebe, A. Auer, and D. Garbe-Schönberg (2011), Surface ocean iron fertilization: The role of airborne volcanic ash from subduction zone and hot spot volcanoes and related iron fluxes into the Pacific Ocean, *Global Biogeochem. Cycles*, *25*, GB4001, doi:10.1029/2009GB003761.

[1]Dynamics of the Ocean Floor Division, Leibniz-Institute of Marine Sciences, IFM-GEOMAR, Kiel, Germany.
[2]Marine Biogeochemistry Division, Leibniz-Institute of Marine Sciences, IFM-GEOMAR, Kiel, Germany.
[3]A. P. Møller Skolen, Upper Secondary School and Sixth Form College of the Danish National Minority in Northern Germany, Schleswig, Germany.
[4]Plymouth Marine Laboratory, Plymouth, UK.
[5]Environment Department, University of York, York, UK.
[6]CO2CRC, Australian School of Petroleum, University of Adelaide, Adelaide, Australia.
[7]Institute of Earth Sciences, University of Iceland, Reykjavik, Iceland.
[8]Departamento de Vulcanología, Instituto de Geofísica, Universidad Nacional Autónoma de México, Coyoacan, Mexico.
[9]Department of Geology, University of Otago, Dunedin, New Zealand.
[10]Institute of Geosciences, Universtity of Kiel, Kiel, Germany.

0886-6236/11/2009GB003761

1. Introduction

[2] Iron (Fe) is a key micronutrient, essential for phytoplankton biochemical processes such as photosynthesis and nitrogen fixation [*Morel and Price*, 2003]. Marine primary production (MPP) is limited by Fe deficiency in High-Nutrient Low-Chlorophyll (HNLC) regions that cover about 40% of the oceans and are mainly located in the subarctic Pacific, the eastern equatorial Pacific, and the Southern Ocean [*Watson*, 2001]. Recent mesoscale Fe fertilization experiments have demonstrated that an increase in dissolved Fe concentration by a few nanomolars in Fe-limited oceanic regions can trigger large-scale diatom blooms [*Behrenfeld et al.*, 1996; *Boyd et al.*, 2000; *Coale et al.*, 1996; *Cooper et al.*, 1996; *Martin and Fitzwater*, 1988; *Turner et al.*, 1996; *Wells*, 2003]. Moreover, addition of Fe to the surface ocean may enhance bacterial nitrogen fixation and contribute

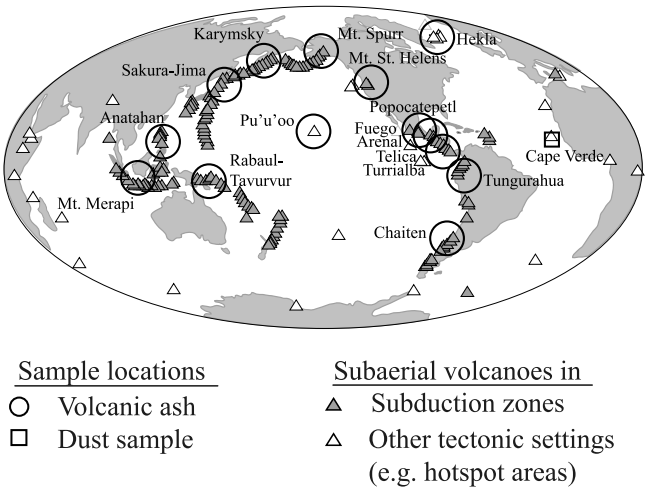

Figure 1. World map showing the provenance of pristine volcanic ash and dust samples used in this study. Also shown is the distribution of subaerially active volcanoes based on the work of *Sigurdsson et al.* [2000].

to N fertilization in open oceanic areas deficient in fixed nitrogen [*Moore et al.*, 2009; *Morel et al.*, 2003]. Changes in surface ocean Fe concentrations can therefore play an important role in the ocean-atmosphere exchange of the greenhouse gas CO_2 both through short-term and long-term effects [*Langmann et al.*, 2010; *Martin et al.*, 1994; *Martin and Fitzwater*, 1988; *Martin et al.*, 1990, 1991; *Watson et al.*, 1991]. Enhancement of the MPP through Fe fertilization may also produce additional biogenic dimethyl sulfide (DMS) and organic carbon (OC), which upon release into the atmosphere impact on the formation and distribution of clouds, and thus on atmospheric albedo [*Lohmann and Feichter*, 2005; *Moore et al.*, 2009; *O'Dowd et al.*, 2004; *Turner et al.*, 2004].

[3] The concentration of Fe in vast areas of the surface ocean is very low [*Boyd et al.*, 2007, 2000; *Coale et al.*, 2004; *De Baar and De Jong*, 2001; *Liu and Millero*, 2002]. The marine deposition of atmospherically transported dusts from deserts or of anthropogenic and extraterrestrial origin has been recognized an important source of soluble (and bioavailable) Fe for the surface ocean [*Jickells and Spokes*, 2001; *Johnson*, 2001; *Mahowald et al.*, 2009; *Sedwick et al.*, 2007]. The role of airborne volcanic ash in supplying Fe to the oceans, however, was poorly constrained despite a suggestion almost 20 years ago that it may well be significant [*Spirakis*, 1991]. Recent studies demonstrate that volcanic ash fallout can significantly raise surface ocean Fe levels [*Censi et al.*, 2010; *Duggen et al.*, 2007, 2010; *Frogner et al.*, 2001; *Jones and Gislason*, 2008] and has the potential to trigger large-scale phytoplankton blooms in Fe-limited (HNLC) oceanic regions [*Hamme et al.*, 2010; *Langmann et al.*, 2010] and eventually affect the marine food web [*Hamme et al.*, 2010]. Moreover, several authors have argued that surface ocean Fe fertilization through major volcanic eruptions led to atmospheric CO_2 drawdowns in the younger part of the Earth's history [*Bay et al.*, 2004; *Cather et al.*, 2009; *Delmelle et al.*, 2009; *Langmann et al.*, 2010; *Sarmiento*, 1993; *Watson*, 1997]. For a recent review of the possible role of volcanic ash for the marine biogeochemical Fe cycle the reader is referred to the work of *Duggen et al.* [2010].

[4] The Pacific Ocean is the largest of the ocean basins and covers about 70% of the Fe-limited oceanic regions. It is encircled by multitudinous active and explosive volcanoes (the Pacific Ring of Fire) and also hosts numerous hot spot volcanic ocean islands (Figure 1). In the Pacific region, at least 50–60 volcanoes are erupting each year and more than 1,300 erupted in the past 10,000 years (http://www.volcano.si.edu/world/). Major eruptions (e.g., Pinatubo 1991) are episodic events from an annual to centennial timescale point of view. Over much longer, geological timescales can the ash input into the Pacific Ocean, which is surrounded by thousands of volcanoes that were active in the Quaternary, be regarded a quasi-continuous process. The flux of volcanic ash into the Pacific Ocean is thus a key parameter in evaluating the significance of Fe flux linked to volcanic ash deposition but has not been constrained until this study.

[5] This paper aims at improving our understanding of the relative importance of volcanic ash as an atmospheric Fe source for the surface ocean. Specifically, our objectives are to (1) produce a robust data basis for the seawater Fe solubility (focusing on the dry deposition process) of pristine volcanic ash from different tectonic settings, (2) constrain the possible regional impact on the surface ocean Fe budget within the ash fallout area of major volcanic eruptions, and (3) improve our understanding of the significance of volcanic ash deposition for the Pacific surface ocean marine biogeochemical Fe cycle.

2. Samples and Methods

[6] The 44 pristine (unhydrated) volcanic ash and one dust sample(s) used in this study were collected from the ground due after deposition and stored dry in plastic bags. The volcanic ash samples were collected fresh shortly (i.e., a couple of hours to 1–2 days) after the eruption in order to prevent Fe-bearing soluble salt coatings to be washed away by rain. Contact with Fe-containing material was avoided (e.g., sieving with metal sieves). The provenance and age of the ash samples is described in more detail in Table S1 in the auxiliary material.[1]

[7] The subduction zone volcanic ash (SZVA) samples stem from 14 different volcanoes in the Pacific Ring of Fire: Sakura-jima (5 samples), Tungurahua (1 sample), Arenal (4 samples), Fuego (1 sample), Turrialba (1 sample), Mt. St. Helens (1 sample), Karymsky (10 samples), Popocatépetl (8 samples), Anatahan (1 sample), Rabaul-Tavurvur (3 samples), Mt. Merapi (1 sample), Chaitén (2 samples), Telica (1 sample), and Mt. Spurr (1 sample). The hot spot volcanic ash (HSVA) samples were collected from 2 different volcanoes: Hekla (3 samples) and Pu'u'oo (1 sample). Locations of the volcanoes are shown in Figure 1, and a detailed description of the ash samples is provided in Table S1. The mineral dust sample was collected on July 2007 from loess deposits (aerosols transported from Sahara) in Calhua (Figure 1) located in the northwestern part of the Cape Verdian island Sao Vicente (16.9°N, 24.9°W). The sample was collected from ground, sieved through 100 μm plastic

[1] Auxiliary materials are available in the HTML. doi:10.1029/2009GB003761.

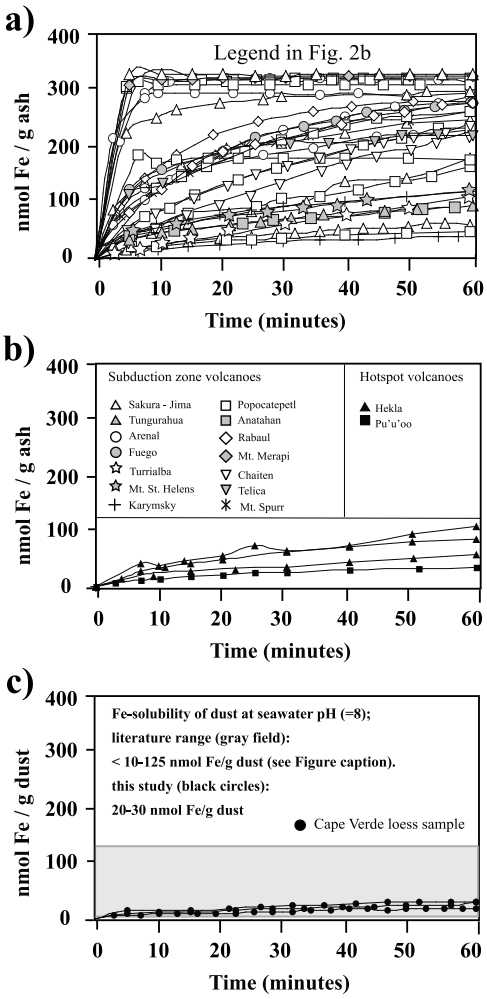

Figure 2. Fe release of (a) subduction zone volcanic ash (SZVA), (b) hot spot volcanic ash (HSVA), and (c) Cape Verde loess sample on contact with natural seawater (buffered at pH 8), determined in situ by means of Cathodic Stripping Voltammetry (CSV). Legend for volcanic ash samples is given in Figure 2b. Symbols indicate ash samples from same volcano collected from different eruptions or different collection distances (see also Table S1). Literature data for mineral dust Fe solubility based on the experiments at seawater pH (=8) including the Cape Verdian loess sample from this study fall within the range of <10 to 125 nmol/g dust (gray bar in Figure 2c, also shown in Table 4) (*Guieu and Thomas* [1996], *Spokes and Jickells* [1996], and this study). The literature data are recalculated from the fractional Fe solubilities ($\%Fe_S$ = 0.001%–0.02%) to nmol Fe/g of dust, assuming that 3.5 wt.% of dust is Fe. The calculations are based on the following equation: Fe release in nmol/g dust = ($\%Fe_S \times$ Fe wt.% $\times 10^9$)/(55.85 g Fe/mol).

filters and stored in plastic bags. Based on the elemental analyses [*Heller and Croot*, 2011], the dust sample is mainly composed of silt from Sahara (generally 80%–95% in the region; [*Desboeufs et al.*, 1999]), which is possibly derived from different sources (Mali, Niger, Chad and southern Algeria) and transported by the West African trade wind.

[8] The Fe release experiments with unsieved pristine volcanic ash samples were performed in situ in natural seawater buffered at seawater pH (=8) by using Cathodic Stripping Voltammetry (CSV, Metrohm VA 757) under clean laboratory conditions, using EPPS as pH buffer and organic ligands to avoid adsorption of the released Fe [*Croot and Johansson*, 2000; *Duggen et al.*, 2007]. The seawater used for the experiments was retrieved during the Meteor cruise M68-3 in the eastern equatorial Atlantic, filtered with 0.2 μm membranes immediately after collection and stored in an acid-cleaned polyethylene carboy. Other containers used during the experiment were made of cleaned quartz glass or polytetrafluoroethylene. Dissolved Fe in oxic seawater precipitates quickly through oxidation of the soluble Fe (II) to less soluble Fe (III) [*Millero and Sotolongo*, 1989] and in order to keep Fe in solution, a thiazolyazo compound (TAC) was used as an Fe-binding ligand [*Croot and Johansson*, 2000]. Prior to the measurements, 20 ml of Atlantic seawater were mixed with 20 μl of 10 mM TAC ligand (2-(2-Thiazolylazo)-p-cresol) and 200 μl of 1M EPPS (4-2(hydroxyethyl) piperazine-1-propanesulfonic acid) solutions in a polyethylene cell cup. A known quantity of ash (~50 mg) was then added to the prepared seawater and measurements done every few minutes. The release of Fe from the Cape Verde dust sample was determined in the same way to allow direct comparison with the volcanic ash data. The experimental setup mimics the soluble Fe input from volcanic ash and mineral dust into seawater through dry deposition, which is considered the globally dominant deposition process for atmospheric particles [*Jickells and Spokes*, 2001].

[9] The major elemental compositions of glass shards and matrix glass of twenty SZVA and four HSVA samples were determined by electron microprobe analysis (EMPA, JEOL-JXA-8200). For the measurements, a ~10 mg subsample of pristine ash was sieved to 32–125 μm size using deionized (DI) water. The ash particles were mounted on a tray with resin, polished and analyzed with a beam current of 6 nA and a beam size of 5 μm. Average glass compositions were inferred from ~25 individual measurements.

[10] The bulk Fe content of selected samples (twelve volcanic ash and one mineral dust sample) was analyzed by inductively coupled plasma-optical emission spectrometry (ICP-OES) with a Spectro Ciros SOP in the Geological Institute of Kiel University. Prior to ICP-OES analyses, 100 mg mill-homogenized dry subsamples were digested by a clean acid mixture of 1 ml HNO_3, 3 ml HCl and 4 ml HF.

3. Results

[11] The in situ increase in dissolved Fe concentrations after addition of the ash/dust material into seawater was converted to Fe release in nanomoles per gram of ash or dust. As shown in Figure 2, between 35 to 340 nmol Fe/g ash were released within the first 60 min of contact with seawater, with SZVA generally mobilizing more Fe (40–340 nmol/g ash) than HSVA (35–107 nmol/g ash; see Figures 2a and 2b). These results are in accordance with previous Fe dissolution experiments with SZVA and seawater (10–100 nmol/g [*Duggen et al.*, 2007; *Jones and Gislason*, 2008]). Most of the ash samples displayed a similar pattern of Fe mobilization, with the highest rates occurring within the first 5–15 min. The Cape Verde mineral dust sample shows a similar Fe mobilization pattern, releasing about 20–30 nmol Fe/g

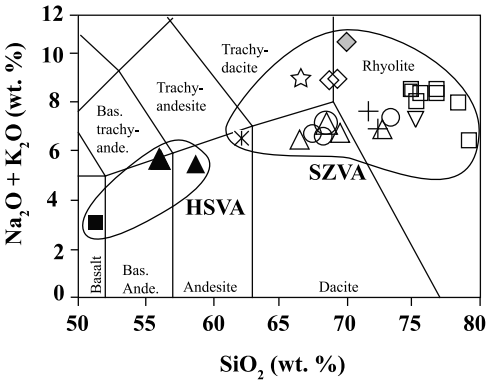

Figure 3. Total silica versus alkali diagram [*Le Bas*, 1984] used to classify volcanic ash samples based on the major element concentrations of glass shards, determined by electron microprobe.

dust (Figure 2c) and falls within the range of mineral dust Fe release data compiled from the literature (Table 4). The external precision of the measurements was calculated from repeat analysis of subsamples (Arenal'93 (n = 2): ~2% deviation, Sakura-jima'86 (n = 2): 44%, Sakura-jima'87 (3 samples): 54% (σ = 47); Cape Verde dust (n = 3): 24% (σ = 7)). The range in reproducibility most likely primarily results from heterogeneity of the samples (e.g., due to particle size distribution, lithic content). The data from the Fe solubility experiments are presented in Table S2.

[12] Based on the total alkali versus silica diagram in Figure 3, the glass compositions range from andesitic to rhyolitic (SZVA) and from basaltic to andesitic (HSVA). The Fe content of the volcanic glass shards ranges from 1 to 11 wt.%, with significantly lower values for SZVA compared to HSVA samples. The major element data of volcanic glass (expressed as element oxides in wt.%) are presented in Table S3.

[13] The total Fe content of the bulk volcanic ash samples range from 1.2 to 8.0 wt.% and deviates from the Fe content of the glass contained in the same sample (Table 1). The Fe content of the Cape Verde dust sample is 6.5 wt.% (Table 1), which is in agreement with results from previous studies with the dust samples from Cape Verde (7.6 wt.%) [*Desboeufs et al.*, 2001, 1999].

4. Discussion

4.1. Fe Solubility of Volcanic Ash: Dissolution Rates and Sources of Soluble Fe

[14] The timescale at which the soluble and thus potentially bioavailable Fe that is released from volcanic ash (Figure 2a) is similar to the timescale at which ash particles sink through the photic zone of the surface ocean: few minutes for coarse (2000–500 μm), to 1–2 h for intermediate (250–150 μm), and to 1–2 days for fine (<50 μm) ash particles (based on Stokes' law estimates [*Duggen et al.*, 2007]). Shorter residence times of about 1–2 h may arise for aggregates of ash particles formed during the humid eruption conditions (e.g., ~1750 m/d for Pinatubo 1991 ash [*Wiesner et al.*, 1995]). Volcanic ash is a mixture of various particles or components with <2 mm diameter that potentially may release Fe on contact with seawater and on different timescales, such as glass shards (quenched magma fragments), pyrogenic minerals (i.e., silicates and oxides), lithic particles (e.g., eroded rock material from the volcanic conduit of any origin) [*Fisher and Schmincke*, 1984; *Óskarsson*, 1981].

[15] The surface of the ash particles are coated by a thin layer of salts in the form of Fe sulfates and Fe halides that are formed through the interaction of ash particles with volcanic gases (S, HCl and HF) and aerosols in the eruption plume [*Delmelle et al.*, 2007; *Naughton et al.*, 1976; *Óskarsson*, 1980, 1981; *Rose*, 1977]. Although Fe content of these salts is still unknown, they are likely to be the most soluble components during seawater dissolution of ash particles [*Duggen et al.*, 2007, 2010; *Frogner et al.*, 2001; *Jones and Gislason*, 2008]. Volcanic glass shards on the other hand usually dominate the bulk composition and can have Fe contents ranging from <1 wt.% to well above 10 wt.% (e.g., Figure 4a; 1–5 wt.% for SZVA and 8–11 wt.% for HSVA). Fe content of pyrogenic minerals ranges from trace to major element level; from basically almost zero (e.g.,

Table 1. Fractional Fe Solubility (%) of Selected Volcanic Ash Samples and Cape Verde Dust[a]

Sample Name	Fe Release Into Seawater (nmol/g Sample)	Total (Bulk) Fe Content (wt.%)	$\%Fe_S^{bulk\ VA}$ or $\%Fe_S^{bulk\ dust}$	Glass Fe Content (wt.%)	$\%Fe_S^{VA\ glass}$
Sakura-Jima 1986	61	5.1	0.007	2.8	0.01
Sakura-Jima 1987	134	4.8	0.02	4.0	0.02
Sakura-Jima 1999	245	4.8	0.03	4.4	0.03
Sakura-Jima 2007	296	5.2	0.03	3.0	0.05
Arenal 1992	227	5.5	0.02	4.4	0.03
Arenal 1993	307	4.7	0.04	5.0	0.03
Arenal 2004	293	4.3	0.04	2.8	0.06
Popocatepetl 2000-1	230	3.7	0.03	1.6	0.08
Popocatepetl 2000-2	314	4.0	0.04	1.0	0.2
Rabaul 2002-1	278	4.6	0.03	2.8	0.06
Chaiten 2008	239	1.2	0.1	1.0	0.1
Hekla 1947	57	8.0	0.004	11.0	0.003
Cape Verde Dust	25	6.5	0.002	no glass	No glass

[a]The fractional Fe solubilities ($\%Fe_S$) are calculated from the Fe release and total Fe of the bulk samples ($\%Fe_S^{bulk}$) or volcanic glass shards contained in the ash samples ($\%Fe_S^{VA\ glass}$) (see auxiliary material). The calculations are based on the following equation: $\%Fe_S$ = (DFe/TFe) × 100; where DFe is the dissolved Fe ((Fe release nmol/g) × (55.85 ng Fe/nmol Fe) × (10^9 g/ng)), and TFe is the total Fe content of bulk ash, dust, and volcanic glass shards (Fe wt.%/100).

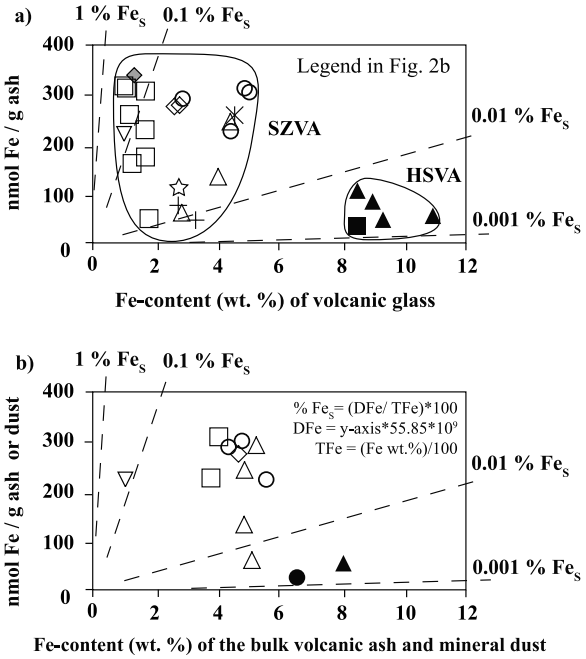

Figure 4. Diagrams display the (a) seawater Fe release of volcanic ash versus the Fe content of volcanic glass shards and (b) seawater Fe release of volcanic and mineral dust versus the total Fe content. Dashed lines show the hypothetical fractional Fe solubilities (%Fe$_s$) ranging from 0.001% to 1% (%Fe$_s$ = (Dissolved Fe/Total Fe)*100).

plagioclase) through 10–30 wt.% FeO (e.g., clinopyroxene) to up to 50–70 wt.% (e.g., magnetite) [*Nakagawa and Ohba*, 2003].

[16] The relation between the total iron and the dissolved iron from volcanic ash is shown in Figure 4. As illustrated in Figure 4, no correlation exists between the Fe release (or Fe solubility) and the Fe content of the volcanic glass or bulk ash samples. Ash samples with lower glass Fe content (<6 wt.%) generally release more soluble Fe than the samples with higher Fe content (>8 wt.%) (Figure 4). Although the salt coatings make up less than 1% of the mass of the bulk sample the data, Figure 4a suggests that very rapid (minute-to-hour scale) release of Fe from ash is most likely dominated by swift dissolution of the surface salts rather than the glass shards, which is in accordance with what was argued in previous studies [*Duggen et al.*, 2007; *Frogner et al.*, 2001; *Jones and Gislason*, 2008]. A recent study with Etna volcanic ash suggests that initial alteration of glass shards and mineral particles may also partly contribute to rapid Fe release [*Censi et al.*, 2010]. On longer timescales (days through weeks to years), alteration of volcanic ash particles deposited as an ash layer at the seafloor is controlled by their bulk chemical composition and may significantly contribute to the surface ocean marine biogeochemical Fe cycle through upwelling.

[17] For the aerosol samples collected over the Pacific Ocean a trend of increasing Fe solubility with decreasing Fe content was reported [*Zhuang et al.*, 1992] similar to what is found for volcanic ash (Figure 4). This trend can be linked to the low Fe contents (or low abundances) of the relatively more dissolvable Fe components. Due to their high Fe contents iron (hydro)-oxides (e.g., hematite, magnetite 60–80 wt.% Fe) are commonly assumed to be the major sources of iron into the surface ocean [*Mahowald et al.*, 2009]. However, it has recently been found that clay minerals are much more soluble although they contain relatively less Fe (<3%–20% Fe) [*Journet et al.*, 2008]. The lack of a correlation between total Fe and the dissolved Fe thus demonstrates that the seawater Fe solubilities of volcanic ash or mineral dust cannot be inferred from the total Fe content but has to be determined directly. Either total iron or the dissolved fraction is not constant rather changing progressively during the long-range transport in the atmosphere. Particle size distribution [*Baker and Jickells*, 2006], mineral composition (aeolian fractionation [*Duggen et al.*, 2010]), and the particle-surface chemistry (chemical and photochemical atmospheric processes [*Duggen et al.*, 2010; *Jickells and Spokes*, 2001; *Spokes and Jickells*, 1996]) may enhance the solubility and bioavailability of Fe in the oceans.

[18] Sample storage is another factor that possibly may affect the Fe mobilization behavior in laboratory experiments. The soluble Fe salts on volcanic ash particles are likely to be unstable and may be affected by storage duration of the sample. Based on the reanalysis of a single ash sample, *Jones and Gislason* [2008] argued that aging of ash material during storage might reduce the Fe release. As inferred from our new data in Figure 5, ash samples stored for more than 10–20 years tend to release less Fe on contact with seawater than younger samples. Five ash samples from Sakura-jima volcano even display a negative correlation between their age and the amount of Fe mobilized. If considered an aging effect, the Sakura-jima ash samples point to a decrease in rapid Fe release of about 200 nmol Fe/g ash over the course of 25 years. The data therefore suggest that Fe release data inferred from volcanic ash several or more years old are generally minimum estimates and that data from younger samples is more reliable.

[19] From the larger data set available it can now be inferred (by taking into account the possible aging effect and uncertainties indicated by repeat measurements) that volcanic ash samples generally release between 35 and 340 nmol Fe/g ash, with a mean of about 200 ± 50 nmol Fe/g for SZVA and possibly around 70 nmol Fe/g for HSVA (Figures 2 and 5) during dry deposition into the surface ocean. The percental (or fractional) Fe solubilities (as commonly used for mineral dust) are calculated in order to allow comparison with the previous aerosol Fe solubility studies. The calculations are based on the Fe release data and the total Fe content of the samples as follows: %Fe$_S$ = (Dissolved Fe/Total Fe)*100 (Table 1). Accordingly, the Fe solubility for volcanic ash (VA) ranges from 0.007% to 0.1% (%$Fe_S^{bulk\ VA}$, using the bulk sample data) and from 0.003% to 0.2% ((%$Fe_S^{VA\ glass}$, using the glass data) (Table 1). Since the composition of volcanic ash progressively approaches the composition of the glass shards contained during aeolian fractionation (see *Duggen et al.* [2010] for details), the overall %Fe_S^{VA} can be constrained to 0.003% to 0.2% (Table 4). As the SZVA samples stem from different volcanoes worldwide (Figure 1), the 200 ± 50 nmol Fe/g (0.01%–0.02% Fe$_S$) value is likely to be representative on a global scale (e.g., dry deposition estimate for global models), and, above all, appears to be largely independent of the bulk composition of the ash samples (Figure 4).

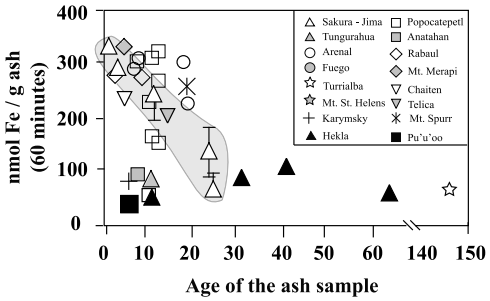

Figure 5. Graph showing the possible influence of storage time on the Fe mobilization behavior of volcanic ash samples. The gray field denotes the correlation between age and Fe release for ash samples from Sakura-jima volcano.

[20] For the Cape Verdian mineral dust sample, the calculated Fe solubility is 0.002% (Table 1). This is in agreement with Fe solubilities reported for other experiments performed at seawater pH (=8) ranging from 0.001% to 0.02% (Table 4) (e.g., 0.001%–0.02% [*Guieu and Thomas*, 1996] and <0.013% [*Spokes and Jickells*, 1996]). The strong dependency of Fe solubilities on the experimental setup with different starting materials and different solutions (e.g., aerosol versus soil samples, pH 4 versus pH 8 solutions) is discussed in section 4.4.

4.2. Regional Impact of Major Volcanic Eruptions on Surface Ocean Fe Concentrations

[21] For a case study of the regional impact a single major eruption we chose a well-constructed historical eruption of Barva volcano in the Central American subduction zone (Figure 6). The Barva eruption deposited at least 7.9×10^{16} g of ash that traveled at least 1000 km distance into the eastern

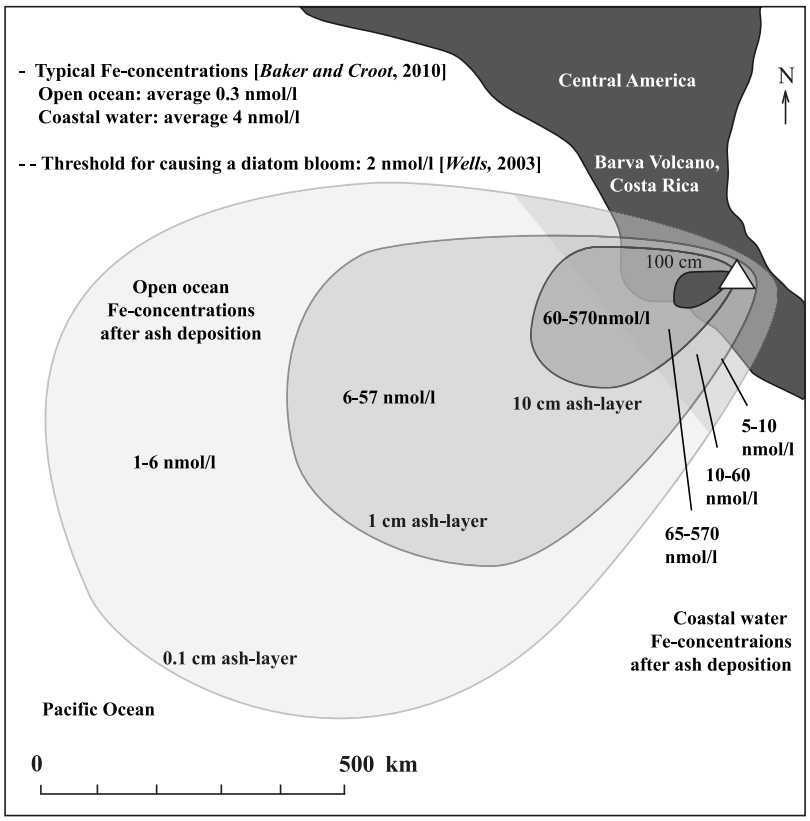

Figure 6. Map showing the extent and particle load in an ash fallout area during a large-scale volcanic eruption, exemplified by the historical Barva eruption (~322,000 years ago) in Costa Rica. Isopachs (ash thickness contours) were mapped on the basis of marine sediment core data [*Kutterolf et al.*, 2008]. Fe concentrations (nmol/L) between the isopachs display the surface ocean Fe levels (100 m mixed layer depth) with ash loads decreasing with increasing distance from the volcano. The Fe levels were inferred from adding the calculated increase in dissolved Fe that is associated with an ash layer of a given thickness (using an average ash density of 2400 kg/m^3 at 30% porosity over 1 dm^2 surface area) to the background seawater Fe levels in coastal waters (typically 4 nmol/L) and the open ocean (typically 0.3 nmol/L) [*Baker and Croot*, 2010; *De Baar and De Jong*, 2001; *Parekh et al.*, 2005]. The range of Fe concentrations originates from the variations in Fe release of volcanic ash (35–340 nmol/g ash, Figure 2). As an example, the maximum increase in Fe concentrations in the open ocean during the deposition of 1 mm ash layer was calculated as follows:[0.3 nmol/L] + [((2400 g/dm^3 − (2400 g/dm^3 × 0.3)) × (1 dm^2 × 0.01 dm) × (340 nmol Fe/g ash)/(1000 dm × 1 dm^2)] = 6 nmol.

equatorial Pacific Ocean [*Kutterolf et al.*, 2008]. Sediment core data allowed the reconstruction of the distribution of the ash layer as well as the thickness that decreases from coast (up to 100 cm thick) to the remote ocean (<1 mm thick) (Figure 6). Assuming an ash density of 2400 kg/m^3 at 30% porosity, ash layer thicknesses of 10 cm, 1 cm and 0.1 cm are recalculated to ash loads of ~170 kg/m^2, ~17 kg/m^2 ~1.7 kg/m^2, respectively.

[22] Volcanic ash fallout impact the surface ocean Fe concentrations depending on the initial seawater Fe concentrations prior to ash deposition, the Fe mobilization behavior of volcanic ash, ash load (ash-to-seawater ratio), the mixed layer depth, and the maximum concentration solubility of iron in seawater [*Baker and Croot*, 2010; *Duggen et al.*, 2010]. In coastal waters, due to higher riverine and continental input, the surface ocean dissolved Fe levels are relatively high and range from 1 to 100 nmol/L with typical concentrations between 8 and 10 nmol/L [*Baker and Croot*, 2010; *Boyd et al.*, 2007, 2000; *Coale et al.*, 2004; *De Baar and De Jong*, 2001; *Liu and Millero*, 2002]. Due to high background levels Fe is generally not limiting phytoplankton growth in coastal waters, although exceptions such as the California upwelling region have been reported [*Hutchins and Bruland*, 1998]. Assuming an initial Fe concentration of about 4 nmol/L in coastal seawater, deposition of a 0.1 cm, 1 cm and 10 cm ash layer with the range in Fe mobilization (shown in Figure 2; 35–340 nmol Fe/g ash) could raise the dissolved Fe concentrations to about 5–10 nmol/L, 10–60 nmol/L, and 65–570 nmol/L, respectively (Figure 6). The inferred values are in accordance with strongly enhanced Fe levels determined in Mediterranean seawater (~600–700 nmol/L) close to Sicily within the ash fallout area of the 2001 eruption of Etna volcano [*Censi et al.*, 2010].

[23] High particle loadings in the close vicinity of a volcanic source may cause increased Fe scavenging of the particles (as seen in the mineral dust deposition [*Baker and Croot*, 2010; *Guieu et al.*, 1997; *Spokes and Jickells*, 1996]) but the distinction of the release versus scavenging is hard to determine. The excess concentrations of dissolved Fe that are above the typical maximum Fe solubility in coastal areas (8–10 nmol/L) would most likely include a large colloidal phase, which is also potentially bioavailable and important to the overall Fe cycling. High Fe levels of several tenths to hundreds nmol/L as observed during the 2001 Etna eruption were argued to be linked to enhanced organic complexation, resulting from lysis of phytoplankton cells during a phytoplankton bloom associated with volcanic ash fallout [*Censi et al.*, 2010]. The short residence time of Fe of about 2–3 months in the surface ocean, however, may limit the biogeochemical impact of volcanic eruptions.

[24] In the surface open ocean, Fe concentrations are extremely low (0.02–0.8 nmol/L) (Figure 7a) thereby limiting phytoplankton growth in HNLC areas [*De Baar and De Jong*, 2001; *Parekh et al.*, 2005]. Assuming an initial Fe concentration for the upper ocean of about 0.3 nmol/L, deposition of a 0.1 cm, 1 cm and 10 cm ash layer could increase Fe levels to about 1–6 nmol/L (at 1000 km distance from the volcano), 6–57 nmol/L (up to 500 km away), and 60–570 nmol/L (up to 250 km from the volcano), respectively (Figure 6). Mesoscale Fe fertilization experiments show that an increase of Fe levels by only 2 nmol/L can stimulate massive diatom blooms in Fe-limited oceanic regions [*Wells*, 2003]. Therefore, even relatively low ash loads corresponding to millimeter-scale ash layers may be sufficient to cause a vigorous MPP response. Based on satellite data a recent study demonstrated a causal connection between the 2008 Kasatochi eruption in the Aleutians and a large scale (~3500 km by 1500 km), about 2–3 months lasting phytoplankton bloom in the subarctic North Pacific [*Hamme et al.*, 2010; *Langmann et al.*, 2010].

4.3. Flux of Volcanic Ash and Mineral Dust Into Pacific Ocean: Millennial-Scale Deposition Rates

[25] The flux of Fe into the Pacific Ocean can be constrained by combining Fe release with geological flux data. Although most of the explosive active volcanoes on Earth are located around the Pacific Ocean that hosts about 70% of the Fe-limited oceanic regions (Figure 7a), an estimate of the airborne volcanic ash input into the Pacific Ocean is so far not available in the literature. Below we therefore constrain the input of airborne volcanic ash into the Pacific, followed by an estimate of the volcanic ash soluble Fe flux, which is then compared with the Fe flux associated with Pacific mineral dust deposition.

[26] The volcanic ash flux into the Pacific Ocean can be considered constant and quasi-continuous over geological timescales, such as the past several 100 ka [*Straub and Schmincke*, 1998], and millenial mineral dust deposition can be considered largely constant after the last glaciation [*Jickells and Spokes*, 2001]. A meaningful way to compare the fluxes of volcanic ash and mineral dust, despite the differences in episodicity/seasonality of deposition, is therefore to recalculate mass and hence Fe fluxes to a postglacial millennial base. Being aware of the uncertainties and limitations of such global-scale estimates, the main goal is to constrain the order of magnitude of Fe release from volcanic ash compared to that of mineral dust, which will be useful to further improve our understanding of the potential role of volcanic ash deposition for the surface Pacific Ocean biogeochemical Fe cycle.

4.3.1. Volcanic Ash Flux Into the Pacific Ocean: Millennial-Scale Estimates

[27] Due to their different nature in eruption style two different approaches are advanced for estimating the fluxes of SZVA and HSVA: (1) an arc-length-based approach for subduction zone (SZ) volcanoes and (2) an apron-based approach for hot spot volcanoes (HS). In both cases we first estimate the amount of ash emitted from Pacific volcanoes and then the fraction that was deposited offshore into the Pacific Ocean. The flux estimates are briefly summarized below and outlined in more detail in Tables 2 and 3.

4.3.1.1. Subduction Zone Volcanic Ash Flux: Arc-Length-Based Approach

[28] Large (strato-)volcanoes, which are the sites of intermediate to major explosive volcanic eruptions, are generally found at nearly constant distances of about 60–100 km apart from each other. Therefore, the length of a subduction zone segment (arc) can be considered proportional to its potential volcanic intensity and thus emitted material flux [*Sigurdsson et al.*, 2000]. The inferred ash flux per millennia and kilometer arc length of any active subduction zone can thus, as a first-order approximation, be applied to any other subduction zone segment in the Pacific.

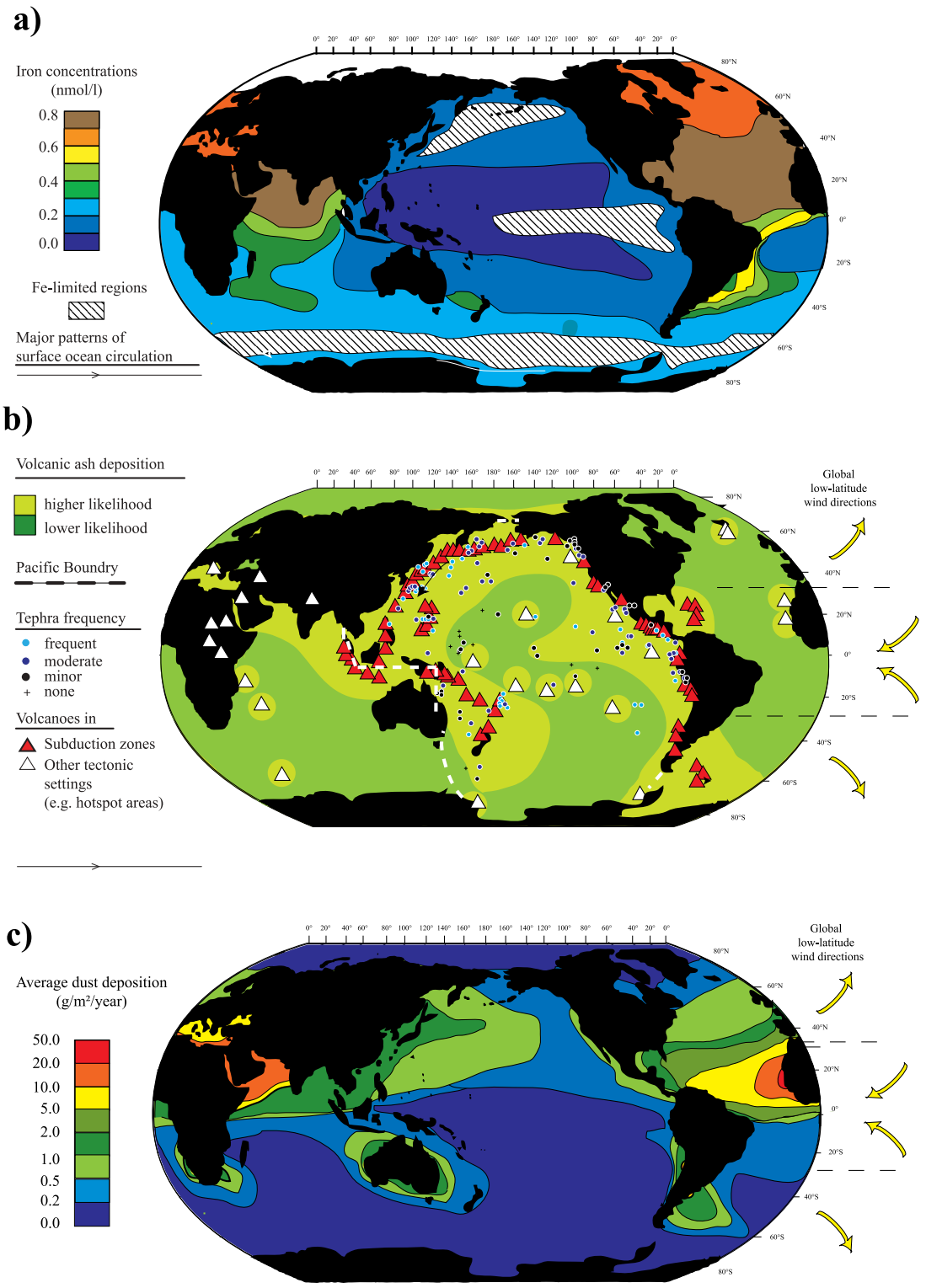

Figure 7. (a) Average surface ocean iron concentrations based on the work of *Parekh et al.* [2005]. High-Nutrient Low-Chlorophyll (HNLC) regions are defined by comparison of the seasonally averaged surface nitrate and silica concentrations [*Watson*, 2001] and annual averaged chlorophyll concentrations (SeaWIFS). (b) Areas of higher versus lower likelihood of volcanic ash deposition, the extent of which are roughly estimated on the basis of the location of historically active volcanoes, low-altitude wind directions, and tephra frequencies in marine sediment drill cores in the Quarternary [*Straub and Schmincke*, 1998]. (c) Averaged annual mineral dust fluxes into the world ocean. Percentage inputs are as follows: North Pacific, 15%; South Pacific, 6%; Southern Ocean, 6%, North Atlantic, 43%; South Atlantic, 4%, and Indian Ocean, 25% [*Jickells et al.*, 2005].

Table 2. Millennial Volcanic Ash Input From Subduction Zone Volcanoes Into the Pacific Ocean

Subduction Zone Volcanic Arcs	Arc Length (km)	Volcanic Ash Emission (10^{15} g/ka)[a]		Offshore Fraction of Emitted Volcanic Ash (%)[b]	Offshore Deposited Volcanic Ash Into the Pacific Ocean (10^{15} g/ka)[c]	
		Min	Max		Min	Max
New Zealand–Tonga-Kermadec	2500	20.0	26.0	85 ± 5	16.0	23.4
Fiji Islands	340	2.7	3.5	85 ± 5	2.2	3.2
New Hebrides	1450	11.6	15.1	85 ± 5	9.3	13.6
Solomon Islands	390	3.1	4.1	85 ± 5	2.5	3.7
New Britian	1000	8.0	10.4	85 ± 5	6.4	9.4
Papau New Guinea	950	7.6	9.9	20 ± 10	0.8	3.0
Indonesia	4700	37.6	48.9	20 ± 10	3.8	14.7
Philippines	1610	12.9	16.8	60 ± 10	6.4	11.7
Ryuku Islands	1210	9.7	12.6	60 ± 10	4.8	8.8
Mariana	1500	12.0	15.6	85 ± 5	9.6	14.1
Izu-Bonin	1100	8.8	11.5	85 ± 5	7.0	10.3
Japan	1400	11.2	14.6	85 ± 5	9.0	13.1
Kuril Islands	1350	10.8	14.1	85 ± 5	8.6	12.6
Kamchatka	1000	8.0	10.4	85 ± 5	6.4	9.4
Aleutians	1900	15.2	19.8	85 ± 5	12.2	17.8
Alaska	800	6.4	8.3	40 ± 10	1.9	4.2
North Canadian Cascades	450	3.6	4.7	20 ± 10	0.4	1.4
High Cascades	1300	10.4	13.5	20 ± 10	1.0	4.1
Mexico	970	7.8	10.1	40 ± 10	2.3	5.0
Central America	1100	8.8[d]	11.5[e]	80 ± 10[f]	6.2	10.3
South America (North)	550	4.4	5.7	80 ± 10	3.1	5.2
South America (Central)	960	7.7	10.0	80 ± 10	5.4	9.0
South America (South)	1300	10.4	13.5	20 ± 10	1.0	4.1
Subduction zone total	29830	239	311	64 ± 8	126	212

[a]Calculated by multiplying maximum and minimum ash emissions (see footnotes d and e).
[b]Estimated on the basis of the general wind directions and proximity of volcanoes to the ocean (see section 4.3.1.1 for explanation).
[c]Calculated by multiplying the result found in footnote a by the estimate from footnote b.
[d]Minimum ash emission from Central American Volcanic Arc (CAVA) over the past 191 ka, calculated on the basis of the work of *Kutterolf et al.* [2008]. The minimum rate of volcanic ash emission per kilometer arc corresponds to 8.0×10^{12} g/ka/km.
[e]Maximum ash emission from CAVA per millennia, estimated by adding the dispersed ash fraction of 30% [*Scudder et al.*, 2009]. The maximum rate of volcanic ash emission per kilometer arc corresponds to 10.4×10^{12} g/ka/km.
[f]Estimated by comparison of proximal and distal ash volumes produced from Central American Arc (see section 4.3.1.1 for explanation).

[29] As a basis for our flux estimates we use the Central American Volcanic Arc (CAVA), which is among the most well-studied subduction zone segments in the Pacific Ring of Fire, with data for offshore deposited ash available for the past 191 ka. Volume estimates of CAVA ash deposits were obtained by fitting straight lines to data on plots of ln isopach thickness versus square root isopach area (e.g., Figure 6) [*Fierstein and Nathenson*, 1992; *Kutterolf et al.*, 2008; *Pyle*, 1989]. It is important to note that the ash volume estimates inferred from discrete ash layers do not account for the dispersed ash, as this fraction is not visible due to mixing with nonvolcanic sediments (e.g., due to bioturbation). The missing dispersed ash fraction corresponds to ~6% to 60% and on average for ~30% of the total erupted mass [*Peters et al.*, 2000; *Rose and Durant*, 2009; *Scudder et al.*, 2009; *Straub and Schmincke*, 1998]. Hence the ash emission rate from CAVA is likely to be underestimated by about 30%.

[30] According to ash thickness contour (isopach) maps inferred from marine drill core data (e.g., Figure 6), about 1139 km^3 of ash was emitted from the 1100 km long CAVA during the past 191 ka (Table S4) [*Kutterolf et al.*, 2008]. By converting volume to mass, this corresponds to about 1680 Pg (Pg = petagrams = 10^{15} grams) of ash for the past 191 ka (using dense rock equivalent densities of 1680 kg/m^3 for mafic and 1470 kg/m^3 for felsic tephra [*Kutterolf et al.*, 2008]). The ash emission rate per millennium can then be calculated to 8.8 Pg/ka and to a rate per kilometer arc of 8.0 Tg/ka/km (Tg = teragrams = 10^{12} grams) (Table 2). Taking into account the dispersed ash fraction (+30%), we infer an ash emission rate of between 8.0 and 10.4 Tg/ka/km for CAVA (Table 2). Assuming that the millennial ash emission rate (per kilometer arc length) is largely the same for all Pacific subduction zone segments, the total emission of all Pacific arcs can be inferred from multiplying the CAVA ash emission rate (of 8.0–10.4 Tg/ka/km) with the known lengths of individual arcs (Table 2). The millennial ash emission for Pacific SZ volcanoes is thus estimated to be on the order of 239–311 Pg/ka (Table 2).

[31] Only a part of the emitted ash is deposited over the ocean. In the case of the well-characterized CAVA, proximal and distal sections of ash layers are found both onshore and offshore (e.g., Figure 6) (Table S4). Based on the interception of proximal and distal facies (at ~20–10 cm ash layer thickness [see *Kutterolf et al.*, 2008]) it can be estimated that about 50% (220 Pg) of the proximal and about 90% (1120 Pg) of the distal ash was deposited into the Pacific Ocean over the past 191 ka (Table S4), which corresponds to about 80% ± 10% of the ash emitted from the CAVA (6.2–10.3 Pg/ka). The result is consistent with the location of Central American volcanoes within trade wind

zone and with the frequency of ash layers in marine drill cores offshore Central America (Figure 7b).

[32] For other SZ segments along the Pacific Ring of Fire, the proportion of offshore deposited ash was estimated by taking into account: (1) the general wind directions (e.g., westerlies, trade winds), (2) the overall distance of the volcanoes from the ocean (Figure 7b), and (3) the constraints for onshore and offshore deposition of CAVA ash (Table 1). For example, in the eastern Pacific, ash from SZ volcanoes located in the trade wind area (~30°N to 30°S) is mostly deposited offshore (e.g., 80% ± 10% for the northern section of the South American Arc; see Table 2 and Figure 7b), whereas ash from volcanoes situated in the westerlies (>30°N and >30°S) is dominantly deposited on land (e.g., only 20% ± 10% deposited offshore for the High Cascades; see Table 2 and Figure 7b). The distance of volcanoes from the ocean is generally larger in the eastern Pacific as these are mainly found at continental margins, whereas SZ volcanoes in the western Pacific often form ocean island arcs (Figure 7b). The proportion of the ash deposited offshore thus tends to be higher for island arcs volcanoes, compared to those located at continental margins (e.g., 85% ± 5% for Mariana Islands in the western Pacific; see Table 2). We also take into account the boundary of the Pacific Ocean (Figure 7b). The ash from Indonesian volcanoes located in the trade wind zone, for example, is mainly transported into the Indian Ocean rather than into the Pacific Ocean (only 20% ± 10% into the Pacific although 80% ± 10% is deposited offshore; see Table 2). Together, we infer a SZVA flux into the Pacific Ocean in the range of 126–212 Pg/ka, which takes into account uncertainties arising from the CAVA ash flux estimate, arc lengths and wind directions (Table 2).

4.3.1.2. Hot Spot Oceanic Island Volcanic Ash Flux: Apron-Based Approach

[33] The data basis from scientific ocean drilling is generally insufficient to construct isopach maps of offshore ash layers related to Pacific HS volcanic ocean islands (Figure 7b). In an apron-based approach, two end-member ocean island settings are distinguished: (1) caldera-forming and (2) non-caldera-forming hot spot systems (Table 3). Caldera-forming ocean islands (e.g., Hawaii) potentially create more explosive volcanic eruptions compared to non-caldera-forming ocean islands (e.g., Samoa, Marquesas) [*Lipman*, 2000] (Figure 7b), for which volcanic apron production rates data are provided by the literature: 230,000 km^3 over the past 5.5 my for caldera-forming Hawaii and 10,000 km^3 over the past 5.0 my for non-caldera-forming Samoa [*Duncan and Clague*, 1985; *Lonsdale*, 1975; *Rees et al.*, 1993; *Straub and Schmincke*, 1998]. These values suggest apron production rates of 42 km^3/ka for caldera-forming and 10 km^3/ka for non-caldera-forming ocean islands (Table 3).

[34] Volcanic aprons not only consist of volcaniclastic rocks (e.g., ash, pumice, hyaloclastites) but also of hardrock formed from lava flows etc. [*Rees et al.*, 1993; *Schmincke and Sumita*, 1998]. The volcaniclastic-to-hardrock ratio is estimated to be about 1:3 (e.g., Hawaii [*Wolfe et al.*, 1994]). Applying this ratio to the apron production rates inferred above and by converting volume to mass using dense rock equivalents of 1680 kg/m^3 for mafic tephra (2400 kg/m^3 at 30% porosity), the volcaniclastic emission rates of hot spot-related ocean islands can be calculated to range from 5.7 Pg/ka to 23.7 Pg/ka (Table 3).

[35] Based on the offshore extend and the thickness of ash layers found in Deep Sea Drilling Project (DSDP) cores related to hot spot volcanism [*Kelts and McKenzie*, 1976; *Viereck et al.*, 1985], the proportion of offshore ash compared to total volcaniclastics is estimated to range from 1% to 5%. The offshore ash deposition rates for individual HS oceanic islands are thus calculated to vary between 0.1 Pg/ka to 2.0 Pg/ka (Table 3). Taking into account whether a hot spot-related ocean island is caldera-forming or non-caldera-forming, the offshore ash deposition rate for Pacific oceanic islands is estimated to be between 2.0 Pg/ka and 9.0 Pg/ka (Table 3), which corresponds to <3% of the apron production rates of HS ocean islands. The HS offshore volcanic ash deposition rate is thus significantly lower than that of SZ volcanoes where in general more large-scale explosive eruptions occur (Table 2).

4.3.1.3. Overall Volcanic Ash Flux Into Pacific Ocean

[36] The Pacific millennial ash input from SZ and HS volcanoes through subaerial eruptions is estimated to range from 128 to 221 × 10^{15} g/ka (Table 4), more than 90% of which is derived from SZ volcanoes (Tables 2 and 3). Despite the uncertainties involved in such geological flux estimates (e.g., the CAVA ash flux, wind directions, arc lengths etc.) that may easily introduce a factor 2 error we argue that the ash flux estimate provided here serves well as a first-order approximation. For comparison, our millennial flux estimate for the Pacific Ocean is 15–20 times lower than the amount of material ejected from the large Pinatubo eruption (~8.1 Pg [*Wiesner et al.*, 1995]). Within a week, a single volcanic eruption can deposit similar amounts ash (e.g., Kasatochi 2008 eruption, at least 650 × 10^{12} g ash [*Langmann et al.*, 2010]) to the yearly input of volcanic ash into Pacific Ocean (128–221 × 10^{12} g/yr based on short-term averaged millennial deposition rates). Therefore, the millennial-scale estimates in Tables 2 and 3 are realistic and rather conservative. The largest uncertainty of our estimate, however, is that it does not consider rare supereruptions that occur with a frequency of ≥10,000 years such as the Toba eruption in Sumatra ~74 ka ago that produced about 2000 × 10^{15} g of ash, much of which was deposited into the ocean [*Oppenheimer*, 2002].

4.3.2. Mineral Dust Input Into the Pacific Ocean: Millennial-Scale Flux

[37] About half of the global surface ocean dust flux is deposited into the northwest Pacific Ocean and stems from Asian deserts (Figure 7c) [*Jickells et al.*, 2005; *Jickells and Spokes*, 2001]. Modeling of extrapolated aerosol dust concentrations (from island and coastal collection sites) suggests an annual dust deposition rate of 39–519 × 10^{12} g/y for the Pacific Ocean [*Mahowald et al.*, 2005]. During the last glaciation the dust input was probably 2–20 times higher than during the more humid (and more vegetated) interglacial periods [*Kohfeld and Harrison*, 2001; *Mahowald et al.*, 1999; *Martin et al.*, 1990; *Winckler et al.*, 2008]. The post-glacial global pattern of dust deposition most likely did not change significantly [*Jickells and Spokes*, 2001]. Therefore, assuming a constant annual dust deposition rate in the Holocene, the annual dust deposition rate inferred from modeling [*Mahowald et al.*, 2005] corresponds to a millennial

Table 3. Millennial Volcanic Ash Input From Hot Spot Volcanoes Into the Pacific Ocean

Hot Spot Oceanic Islands	Volcaniclastic Production Rate (10^{15} g/ka)[a]	Offshore Deposited Volcanic Ash Into the Pacific Ocean (10^{15} g/ka)[b]	
		Minimum	Maximum
Hawaii (caldera-forming)	23.7	0.4	2.0
Revillagigedos	5.7	0.1	0.5
Marquesas	5.7	0.1	0.5
Gambier	5.7	0.1	0.5
Society	5.7	0.1	0.5
Austral-Cook	5.7	0.1	0.5
Caroline	5.7	0.1	0.5
Easter hot spot	5.7	0.1	0.5
Galapagos (caldera-forming)	23.7	0.4	2.0
Samoa (non-caldera-forming)	5.7	0.1	0.5
Line Island	5.7	0.1	0.5
Marshall-Gilbert Island	5.7	0.1	0.5
Hot spot total	104	2	9

[a]Volcaniclastic emission rates estimated on the basis of apron production rates of Hawaii (42 km^3/ka over 5.5 myr) and Samoa (10 km^3/ka over 5 myr), and applying the ratio between volcaniclastic to the hardrock (1/3) (see section 4.3.1.2 for explanation) [*Straub and Schmincke*, 1998; *Wolfe et al.*, 1994]. Volumes were converted to masses based on an average mafic ash density of 2400 kg/m^3 at 30% porosity (1680 kg/m^3).

[b]Fraction of offshore ash compared to emitted volcaniclastics is estimated to range between 1%–5% [*Kelts and McKenzie*, 1976; *Viereck et al.*, 1985].

dust flux rate of 39–519 × 10^{15} g/ka. Based on ocean sediment core data, however, the postglacial dust input is estimated to be 4–5 times lower than the modeling estimates [*Rea*, 1994], possibly due to a less anthropogenic input before the past 1000 years.

4.4. Significance of Volcanic Ash-Related Fe Input Into the Pacific Ocean: Biogeochemical Implications, Eruption Frequencies, and Spatial Distributions

[38] The millennial flux of airborne volcanic ash into the Pacific Ocean (128–221 × 10^{15} g/ka) is comparable to that of mineral dust (39–519 × 10^{15} g/ka [*Mahowald et al.*, 2009]) or 50–115 × 10^{15} g/ka if corrected to sediment core observations [*Rea*, 1994] (see Table 4). From the similarity in both material flux and Fe solubilities in seawater at pH = 8 (Table 4) it follows that the flux of soluble Fe through dry deposition of volcanic ash into the Pacific Ocean is comparable to that of mineral dust (3–75 × 10^9 mol Fe/ka for volcanic ash and 1–65 × 10^9 mol Fe/ka for mineral dust). These estimates do not consider the effect of wet deposition (by rainwater) that, based on experimental results, would greatly enhance the Fe solubility of both volcanic ash and mineral dust as shown in Table 4 (see discussion in section 4.1) [*Baker and Croot*, 2010; *Duggen et al.*, 2010; *Mahowald et al.*, 1999]. The ratio of wet to dry deposition may, however, vary from region to region but on a global-scale dry deposition dominates. As outlined by *Jickells and Spokes* [2001] for the Pacific Ocean, about 70% of the atmospheric particles are derived through dry deposition.

[39] Focusing on the dry deposition process, for mineral dust an overall range of 0.001%–0.02% Fe_S is derived based on the experiments (including this study) providing constraints for the solubility of Fe under seawater conditions (e.g., constant pH of 8) (Table 4). Previously, a value of 0.01% Fe_S was chosen for the dry deposition of Fe into the Saragossa Sea [*Jickells*, 1999], which is in accordance with the range outlined in Table 4. Results for Fe solubilities inferred from experiments at highly variable pH vary 3–4 orders of magnitude: 0.001%–22% for volcanic ash and 0.001%–80% for mineral dust (Table 4 and, for comparison with the new data, see the dashed lines in Figure 4) [*Baker and Croot*, 2010; *Duggen et al.*, 2010; *Frogner et al.*, 2001; *Jones*

Table 4. Summary of the Fe Mobilization Behavior of Volcanic Ash and Mineral Dust in Different Experimental Setups With Variable pH and the Input of Soluble Fe Based on the Millennial Fluxes of Volcanic and Mineral Dust

	Volcanic Ash		Mineral Dust	
	nmol/g Ash	$\%Fe_S^{VA}$	nmol/g Dust	$\%Fe_S^{dust}$
Fe Release (nmol Fe/g or % Fe_S)				
At seawater pH (8)	35–340[a]	0.003–0.2[a]	<10–125[b,c]	0.001–0.02[b]
In seawater without pH buffer	10–39,000[d]	0.001–1.8[c,d]	1,600–165,000[c,e]	0.26–26[c]
in acidic solutions (pH 1–5)	20–200,00[f]	0.001–22[c,f]	60–500,000[c,g]	0.01–80[g]
Millennial particle flux into the Pacific Ocean (10^{15} g/ka)	128–221[h]		39–519[i]	
Soluble Fe Flux Into the Pacific Ocean[j] (10^9 mol/ka)				
At seawater pH (8)	3–75		1–65	
In seawater without pH buffer	2–8,600		65–85,000	
In acidic solutions (pH 1–5)	2–44,000		2–260,000	

[a]Values as follows: 20–70 nmol/g ash [*Duggen et al.*, 2007]; and 35–340 nmol/g ash (Figures 2a and 2b) (present study (0.003%–0.2% Fe_S^{VA}; Table 1)).

[b]Values as follows: 0.001%–0.02% Fe_S^{dust} [*Guieu and Thomas*, 1996]; <0.013% Fe_S^{dust} [*Spokes and Jickells*, 1996]; and 20–30 nmol/g ash (Figure 2c) (present study (0.002% Fe_S^{dust}; Table 1)).

[c]Values recalculated from Fe release in "nmol Fe/g" to "%Fe_S" (fractional Fe solubility) and vice versa. Bulk Fe contents are 5% for SZVA, 12% for HSVA, and 3.5% for mineral dust.

[d]Values as follows: 10–10,900 nmol/g ash [*Jones and Gislason*, 2008]; and 39,000 nmol/g ash [*Frogner et al.*, 2001].

[e]*Buck et al.* [2006] and *Wu et al.* [2007].

[f]*Duggen et al.* [2010, and references therein].

[g]*Baker and Croot* [2010], *Mahowald et al.* [2009], and references therein.

[h]This study; estimations based on the drill core data (see section 4.3 and Tables 2 and 3).

[i]Derived from long-term averaged modern deposition rates [*Mahowald et al.*, 2005] (see section 4.3.2 for discussion).

[j]Calculated by multiplying the millennial particle fluxes (g/ka) with the Fe release per gram of ash and dust (nmol Fe/g ash or dust).

and Gislason, 2008; *Mahowald et al.*, 2005; *Schroth et al.*, 2009]. Table 4 emphasizes that major uncertainties in estimating Fe flux arise from the strong pH dependency of Fe solubility. Experimental studies demonstrate this with highest Fe solubilities under low pH with minimum Fe solubilities around pH 8 [*Desboeufs et al.*, 1999; *Guieu and Thomas*, 1996; *Spokes and Jickells*, 1996]. Since results from experiments with acidic solutions are very likely to overestimate the dissolution of Fe in seawater [*Baker et al.*, 2006], our Fe flux estimates for both volcanic ash and mineral dust were performed with data from experiments at seawater pH of 8.

[40] Volcanic ash and mineral dust particles can serve as cloud condensation nuclei (CCN) [*Andreae and Rosenfeld*, 2008; *Duggen et al.*, 2010; *Jickells and Spokes*, 2001; *Textor et al.*, 2006]. Therefore the particles that were transported long distances through the atmosphere may have been affected by interaction with low-pH cloud water prior to dry deposition (soil versus marine aerosol [*Zhuang et al.*, 1992]). The volcanic ash samples used in this study were transported between a few and up to 130 km through the atmosphere (see Table S1), whereas the Cape Verdian loess sample was collected more than 1000 km away from its source. As long-distance atmospheric transportation may enhance Fe solubilities, Fe release data for ash particles sampled in the proximity of volcanic source craters may underestimate actual Fe solubilities in the remote ocean. It is still uncertain to what extend low-pH cloud water cycling of ash and dust particles affects the seawater solubility (hence bioavailability) of Fe. In terms of biogeochemical Fe and C cycles, however, a key parameter is the maximum concentration solubility of Fe that is controlled by various factors (e.g., nature of Fe-binding ligands) and Fe uptake mechanisms by marine photosynthetic organisms which are not completely understood [*Baker and Croot*, 2010].

[41] Due to differences in temporal and spatial deposition patterns, comparable millennial Fe fluxes into the Pacific Ocean are unlikely to have the similar marine biogeochemical impacts (Figure 7). The episodic deposition nature of mineral dust and volcanic ash (e.g., in the northern Pacific) may be less different than commonly thought. Despite its seasonality the dust input into the Pacific is not uniform throughout the year. About 30%–90% of the annual dust input is derived in the vicinity to the dust source at about 5% of the high deposition days [*Mahowald et al.*, 2009]. Episodic dust storms occur about 20% of the days of a year, and may deposit about half of the yearly input within a 2 week period [*Jickells and Spokes*, 2001]. In terms of mass flux, the frequency and duration of the storm events is comparable to the moderate level of volcanic eruptions. Low-to-moderate eruptions (volcanic explosivity index of VEI <5 with ejecta volumes <1 km^3 and ash plume heights of <10–25 km) are episodic but take place frequently. The relatively frequent volcanic eruptions can be grouped into (1) constant-to-daily gentle eruptions (eruption column height of hundreds of meters, e.g., Hawaiian volcanoes), (2) weekly eruptions (1–3 km ash plume height, e.g., Galeras), and (3) yearly explosive eruptions (3–5 km ash plume height, e.g., Cordón Caulle) (http://www.volcano.si.edu/).

[42] Each year at least 25 eruptions of VEI = 2 (<10^{11} grams ash), about 15 eruptions of VEI = 3 (<10^{14} grams ash), and about 1–4 eruptions of VEI = 4 (<10^{15} grams ash) occur along the Pacific Ring of Fire (http://www.volcano.si.edu/). Globally, high-magnitude eruptions with ejecta of >10^{15} grams (with ash plume heights of 10–25 km) occur every ≥10 years (e.g., Eyjafjallajökull 2010 eruption, VEI = 5). Supereruptions with ejecta of >10^{16} grams to >10^{19} grams (with ash plume heights of >25 km) are rare and take place every ≥10 to ≥10,000 years, depending on the magnitude (e.g., Pinatubo 1991, VEI = 6; Tambora 1815, VEI = 7; Taupo ~26,500 years ago, VEI = 8). Fe fertilization that may arise from such large-scale eruptions to supereruptions is to date basically unknown but some studies indicate that the effect may have been significant in the Earth's history [*Duggen et al.*, 2010, and references therein].

[43] In terms of biogeochemical response and C cycles, both sources can be expected to have their greatest impact on Fe-limited (HNLC) regions (Figure 7a) [*De Baar and De Jong*, 2001; *Watson*, 2001]. While mineral dust deposition is mainly restricted to the northwestern Pacific HNLC region (Figures 7a and 7c), Fe input by volcanic ash is more widespread including the north (subarctic), eastern equatorial and southwestern Pacific (Figure 7b). In the subarctic Pacific, for example, the ash fallout of the intermediate-scale August 2008 eruption of Kasatochi volcano (VEI = 4) was associated with a large-scale phytoplankton bloom in the Fe-limited North Pacific [*Hamme et al.*, 2010; *Langmann et al.*, 2010]. In the Fe-limited eastern equatorial Pacific mineral dust input is relatively rare so that the flux of soluble Fe from ash from Mexican, Central American, and South American volcanoes is likely to dominate the millennial atmospheric input of Fe in these regions (Figure 7). In the Pacific sector of the Southern Ocean mineral dust deposition is very limited too, whereas volcanic ash from active volcanoes in the subduction zones of New Zealand and Tonga-Kermadec can be transported into the Fe-limited Southern Ocean with the westerlies, potentially causing volcanic Fe fertilization (Figure 7b).

5. Conclusions

[44] Airborne volcanic ash from volcanoes in different tectonic settings (subduction zones and hot spots) rapidly mobilizes soluble Fe on contact with natural seawater. Calculations suggest that even low ash loads within the ash fallout area of single volcanic eruptions can raise Fe levels sufficiently to cause massive phytoplankton blooms. Flux estimates suggest that the postglacial millennial input of Fe into the Pacific surface ocean through dry deposition of volcanic ash and mineral dust is comparable. Although the millennial Fe fluxes are found to be similar, the biogeochemical impacts of the two atmospheric sources are distinguished by differences in temporal and spatial deposition patterns in the Pacific surface ocean in general and in Fe-limited (HNLC) regions in particular.

[45] Further research to improve our understanding of the relative importance of volcanic ash and mineral dust for the Pacific surface ocean should include an evaluation of the amount of Fe that is transported into the Pacific through dry versus wet deposition, as Fe release of both volcanic ash and mineral dust particles appears to be strongly pH-dependent, and Fe release is strongly enhanced by interaction with low-pH solutes (e.g., cloud water). Despite the uncertainties typically involved in near-global flux estimates and differences in the biogeochemical impact patterns of volcanic ash

and mineral dust, our results strongly suggests that the role of volcanic ash for the Pacific surface ocean biogeochemical Fe cycle is significant and has so far been underestimated.

[46] **Acknowledgments.** We are grateful to L. Lara, C. Wallace, C. Neal, G. Alvarado-Induni, T. Kobayashi, I. Itikar, M. Iguchi, T. Noal, M. Mc Kinon, A. Gerst, and G. J. Dennis for kindly providing ash samples and to M. Heller for providing the dust sample. We greatly appreciate S. Kutterolf's constructive comments. We are thankful to M. Thoener for technical assistance with the electron microprobe analyses and to Ulrike Westernströer and Sabine Lange for their efforts with the ICP-OES analyses. S.D. was supported by the German Research Foundation, DFG (project Ho1833-16). P.D.'s contribution to this project was supported by a Vice Chancellor's Anniversary Lectureship, University of York. The paper is contribution 174 of the Sonderforschungsbereich (SFB) 574 "Volatiles and Hazards in Subduction Zones." The study was made possible by IFM-GEOMAR through in-house funding of the multidisciplinary research group NOVUM "Nutrients Originating Volcanoes and Their Effects on the Euphotic Zone of the Marine Ecosystem."

References

Andreae, M. O., and D. Rosenfeld (2008), Aerosol-cloud-precipitation interactions: Part 1. The nature and sources of cloud-active aerosols, *Earth Sci. Rev.*, *89*, 13–41, doi:10.1016/j.earscirev.2008.03.001.

Baker, A., and P. Croot (2010), Atmospheric and marine controls on aerosol iron solubility in seawater, *Mar. Chem.*, *120*, 4–13, doi:10.1016/j.marchem.2008.09.003.

Baker, A. R., and T. D. Jickells (2006), Mineral particle size as a control on aerosol iron solubility, *Geophys. Res. Lett.*, *33*, L17608, doi:10.1029/2006GL026557.

Baker, A., M. French, and K. L. Linge (2006), Trends in aerosol nutrient solubility along a west-east transect of the Saharan dust plume, *Geophys. Res. Lett.*, *33*, L07805, doi:10.1029/2005GL024764.

Bay, R. C., N. Bramall, and P. B. Price (2004), Bipolar correlation of volcanism with millennial climate change, *Proc. Natl. Acad. Sci. U. S. A.*, *101*, 6341–6345, doi:10.1073/pnas.0400323101.

Behrenfeld, M. J., A. J. Bale, Z. S. Kolber, J. Aiken, and P. G. Falkowski (1996), Confirmation of iron limitation of phytoplankton photosynthesis in the equatorial Pacific Ocean, *Nature*, *383*, 508–511, doi:10.1038/383508a0.

Boyd, P. W., et al. (2000), A mesoscale phytoplankton bloom in the polar Southern Ocean stimulated by iron fertilization, *Nature*, *407*, 695–702, doi:10.1038/35037500.

Boyd, P. W., et al. (2007), Mesoscale iron enrichment experiments 1993–2005: Synthesis and future directions, *Science*, *315*, 612–617, doi:10.1126/science.1131669.

Buck, S. C., W. M. Landing, J. A. Resing, and G. T. Lebon (2006), Aerosol iron and aluminum solubility in the northwest Pacific Ocean: Results from the 2002 IOC cruise, *Geochem. Geophys. Geosyst.*, *7*, Q04M07, doi:10.1029/2005GC000977.

Cather, S. M., N. W. Dunbar, F. W. McDowell, W. C. McIntosh, and P. A. Scholle (2009), Climate forcing by iron fertilization from repeated ignimbrite eruptions: The icehouse–silicic large igneous province (SLIP) hypothesis, *Geosphere*, *5*, 315–324, doi:10.1130/GES00188.1.

Censi, P., L. A. Randazzo, P. Zuddas, F. Saiano, P. Aricò, and S. Andò (2010), Trace element behaviour in seawater during Etna's pyroclastic activity in 2001: Concurrent effects of nutrients and formation of alteration minerals, *J. Volcanol. Geotherm. Res.*, *193*, 106–116, doi:10.1016/j.jvolgeores.2010.03.010.

Coale, K. H., et al. (1996), A massive phytoplankton bloom induced by an ecosystem-scale iron fertilization experiment in the equatorial Pacific Ocean, *Nature*, *383*, 495–501, doi:10.1038/383495a0.

Coale, K. H., et al. (2004), Southern Ocean iron enrichment experiment: Carbon cycling in high- and low-Si waters, *Science*, *304*, 408–414, doi:10.1126/science.1089778.

Cooper, D. J., A. J. Watson, and P. D. Nightingale (1996), Large decrease in ocean-surface CO_2 fugacity in response to in situ iron fertilization, *Nature*, *383*, 511–513, doi:10.1038/383511a0.

Croot, P., and M. Johansson (2000), Determination of iron speciation by cathodic stripping voltammetry in seawater using the competing ligand 2-(2-Thiazolylazo)-*p*-creasol (TAC), *Electroanalysis*, *12*, 565–576, doi:10.1002/(SICI)1521-4109(200005)12:8<565::AID-ELAN565>3.0.CO;2-L.

De Baar, H. J. W., and J. T. M. De Jong (2001), Distributions, sources and sinks of iron in seawater, in *The Biogeochemistry of Iron in Seawater*, edited by D. R. Turner and K. A. Hunter, pp. 212–215, Wiley, Chichester, U. K.

Delmelle, P., M. Lambert, Y. Dufrene, P. Gerin, and N. Oskarsson (2007), Gas/aerosol–ash interaction in volcanic plumes: New insights from surface analyses of fine ash particles, *Earth Planet. Sci. Lett.*, *259*, 159–170, doi:10.1016/j.epsl.2007.04.052.

Delmelle, P., C. Maclean, and J. Calkins (2009), Volcanic ash deposition and phytoplankton growth: A plausible connection, poster presented at *SOLAS Open Science Conference*, SCOR, Barcelona, Spain, 16–19 November.

Desboeufs, K. V., R. Losno, F. Vimeux, and S. Cholbi (1999), The pH-dependent dissolution of wind-transported Saharan dust, *J. Geophys. Res.*, *104*, 21,287–21,299.

Desboeufs, K. V., R. Losno, and J. L. Colin (2001), Factors infuencing aerosol solubility during cloud processes, *Atmos. Environ.*, *35*, 3529–3537, doi:10.1016/S1352-2310(00)00472-6.

Duggen, S., P. Croot, U. Schacht, and L. Hoffmann (2007), Subduction zone volcanic ash can fertilize the surface ocean and stimulate phytoplankton growth: Evidence from biogeochemical experiments and satellite data, *Geophys. Res. Lett.*, *34*, L01612, doi:10.1029/2006GL027522.

Duggen, S., N. Olgun, P. Croot, L. Hoffmann, H. Dietze, and C. Teschner (2010), The role of airborne volcanic ash for the surface ocean biogeochemical iron-cycle: A review, *Biogeosciences*, *7*, 827–844, doi:10.5194/bg-7-827-2010.

Duncan, R. A., and D. A. Clague (Eds.) (1985), *Pacific Plate Motion Recorded by Linear Volcanic Chains*, 89–121 pp., Plenum Press, New York.

Fierstein, J., and M. Nathenson (1992), Another look at the calculation of fallout tephra volumes, *Bull. Volcanol.*, *54*, 156–167, doi:10.1007/BF00278005.

Fisher, R. V., and H.-U. Schmincke (1984), *Pyroclastic Rocks*, 472 pp., Springer, Berlin.

Frogner, P., S. R. Gislason, and N. Óskarsson (2001), Fertilizing potential of volcanic ash in ocean surface water, *Geology*, *29*, 487–490, doi:10.1130/0091-7613(2001)029<0487:FPOVAI>2.0.CO;2.

Guieu, C., and A. J. Thomas (1996), Saharan aerosols: From the soil to the ocean, in *The Impact of Desert Dust across the Mediterranean*, edited by S. Guerzoni and R. Chester, pp. 207–216, Kluwer, Dordrecht, Netherlands.

Guieu, C., R. Chester, M. Nimmo, J. M. Martin, S. Guerzoni, E. Nicolas, J. Mateu, and S. Keyse (1997), Atmospheric input of dissolved and particulate metals to the northwestern Mediterranean, *Deep Sea Res., Part II*, *44*, 655–674, doi:10.1016/S0967-0645(97)88508-6.

Hamme, R. C., et al. (2010), Volcanic ash fuels anomalous plankton bloom in subarctic northeast Pacific, *Geophys. Res. Lett.*, *37*, L19604, doi:10.1029/2010GL044629.

Heller, M. I., and P. L. Croot (2011), Superoxide decay as a probe for speciation changes during dust dissolution in tropical Atlantic surface waters near Cape Verde, *Mar. Chem.*, in press.

Hutchins, D. A., and K. A. Bruland (1998), Iron-limited diatom growth and Si:N ratios in a coastal upwelling region, *Nature*, *393*, 561–564, doi:10.1038/31203.

Jickells, T. D. (1999), The inputs of dust derived elements to the Sargasso Sea; a synthesis, *Mar. Chem.*, *68*, 5–14, doi:10.1016/S0304-4203(99)00061-4.

Jickells, T. M., and L. J. Spokes (2001), Atmospheric iron inputs to the oceans, in *Biogeochemistry of Iron in Seawater*, edited by D. R. Turner and K. Hunter, pp. 85–121, Wiley, Chichester, U. K.

Jickells, T. D., Z. S. An, and K. K. Andersen (2005), Global iron connections between desert dust, ocean biogeochemistry, and climate, *Science*, *308*, 67–71, doi:10.1126/science.1105959.

Johnson, K. S. (2001), Iron supply and demand in the upper ocean: Is extraterrestrial dust a significant source of bioavailable iron?, *Global Biogeochem. Cycles*, *15*, 61–63, doi:10.1029/2000GB001295.

Jones, M. T., and S. R. Gislason (2008), Rapid releases of metal salts and nutrients following the deposition of volcanic ash into aqueous environments, *Geochim. Cosmochim. Acta*, *72*, 3661–3680, doi:10.1016/j.gca.2008.05.030.

Journet, E., K. V. Desboeufs, S. Caquineau, and J. L. Colin (2008), Mineralogy as a critical factor of dust iron solubility, *Geophys. Res. Lett.*, *35*, L07805, doi:10.1029/2007GL031589.

Kelts, K., and J. A. McKenzie (1976), Cretaceous volcanigenic sediments from the Line Island chain: Diagenesis and formation of K-feldspar, DSDP leg 33, site 315 A and site 316, in *Initial Reports of DSDP*, edited by S. O. Schlanger and E. D. Jackson, pp. 789–803, US Govt. Print. Off., Washington, D. C.

Kohfeld, K. E., and S. P. Harrison (2001), DIRTMAP: The geological record of dust, *Earth Sci. Rev.*, *54*, 81–114, doi:10.1016/S0012-8252(01)00042-3.

Kutterolf, S., A. Freundt, and W. Perez (2008), Pacific offshore record of plinian arc volcanism in Central America: 2 Tephra volumes and erupted masses, *Geochem. Geophys. Geosyst.*, *9*, Q02S02, doi:10.1029/2007GC001791.

Langmann, B., K. Zaksek, M. Hort, and S. Duggen (2010), Volcanic ash as fertiliser for the surface ocean, *Atmos. Chem. Phys.*, *10*, 3891–3899, doi:10.5194/acp-10-3891-2010.

Le Bas, M. J. (1984), Nephelinites and carbonatites, *Geol. Soc. Spec. Publ.*, *30*, 53–83.

Lipman, P. W. (2000), Calderas, in *Encylopedia of Volcanoes*, edited by H. Sigurdsson, pp. 645–669, Academic, San Diego, Calif.

Liu, X. W., and F. J. Millero (2002), The solubility of iron in seawater, *Mar. Chem.*, *77*, 43–54, doi:10.1016/S0304-4203(01)00074-3.

Lohmann, U., and J. Feichter (2005), Global indirect aerosol effects: A review, *Atmos. Chem. Phys.*, *5*, 715–737, doi:10.5194/acp-5-715-2005.

Lonsdale, P. (1975), Sedimentation and tectonic modification of Samoan Archipelagic Apron, *Am. Assoc. Pet. Geol.*, *59*, 780–798.

Mahowald, N., K. Kohfeld, M. Hansson, Y. Balkanskси, S. P. Harrison, I. C. Prentice, M. Schluz, and H. Rodhe (1999), Dust sources and deposition during the last glacial maximum and current climate: A comparison of model results with paleodata from ice cores and marine sediments, *J. Geophys. Res.*, *104*(D13), 15,895–15,916, doi:10.1029/1999JD900084.

Mahowald, N. M., A. R. Baker, G. Bergametti, N. Brooks, R. A. Duce, T. D. Jickells, N. Kubilay, J. M. Prospero, and I. Tegen (2005), Atmospheric global dust cycle and iron inputs to the ocean, *Global Biogeochem. Cycles*, *19*, GB4025, doi:10.1029/2004GB002402.

Mahowald, N., et al. (2009), Atmospheric iron deposition: Global distribution, variability, and human perturbations, *Annu. Rev. Mar. Sci.*, *1*, 245–278, doi:10.1146/annurev.marine.010908.163727.

Martin, J. H., and S. E. Fitzwater (1988), Iron deficiency limits phytoplankton growth in the north-east Pacific subarctic, *Nature*, *331*, 341–343, doi:10.1038/331341a0.

Martin, J. H., R. M. Gordon, and S. E. Fitzwater (1990), Iron in Antarctic waters, *Nature*, *345*, 156–158, doi:10.1038/345156a0.

Martin, J. H., R. M. Gordon, and S. E. Fitzwater (1991), The case for iron, *Limnol. Oceanogr.*, *36*, 1793–1802, doi:10.4319/lo.1991.36.8.1793.

Martin, J. H., K. H. Coale, and K. S. Johnson (1994), Testing the iron hypothesis in ecosystems of the equatorial Pacific Ocean, *Nature*, *371*, 123–129, doi:10.1038/371123a0.

Millero, F. J., and S. Sotolongo (1989), The oxidation of Fe(II) with H_2O_2 in seawater, *Geochim. Cosmochim. Acta*, *53*, 1867–1873, doi:10.1016/0016-7037(89)90307-4.

Moore, C. M., et al. (2009), Large-scale distribution of Atlantic nitrogen fixation controlled by iron availability, *Nat. Geosci. Lett.*, *2*, 867–871, doi:10.1038/ngeo667.

Morel, F. M. M., and N. M. Price (2003), The biogeochemical cycles of trace metals in the oceans, *Science*, *300*, 944–947, doi:10.1126/science.1083545.

Morel, F. M. M., A. J. Milligan, and M. A. Saito (2003), Marine bioinorganic chemistry: The role of trace metals in the oceanic cycles of major nutrients, in *Treatise on Geochemistry*, edited by H. Elderfield, pp. 113–143, Elsevier, Oxford, U. K.

Nakagawa, M., and T. Ohba (2003), Minerals in volcanic ash 1: Primary minerals and volcanic glass, *Global Environ. Res.*, *6*, 41–51.

Naughton, J. J., V. A. Greenberg, and R. Googuel (1976), Incrustations and fumarolic condensates at Kilauea Volcano, Hawaii: Field, drill-hole, and laboratory observations, *J. Volcanol. Geotherm. Res.*, *1*, 149–165, doi:10.1016/0377-0273(76)90004-4.

O'Dowd, C. D., M. C. Facchini, F. Cavalli, D. Ceburnis, M. Mircea, S. Decesari, S. Fuzzi, Y. J. Yoon, and J. P. Putaud (2004), Biogenically driven organic contribution to marine aerosol, *Nature*, *431*, 676–680, doi:10.1038/nature02959.

Oppenheimer, C. (2002), Limited global change due to the largest known Quaternary eruption, Toba ≈ 74 kyr BP?, *Quat. Sci. Rev.*, *21*, 1593–1609.

Óskarsson, N. (1980), The interaction between volcanic gases and tephra: Flourine adhering to tephra of the 1970 Hekla eruption, *J. Volcanol. Geotherm. Res.*, *8*, 251–266, doi:10.1016/0377-0273(80)90107-9.

Óskarsson, N. (1981), The chemistry of Icelandic lava incrustations and the latest stages of degassing, *J. Volcanol. Geotherm. Res.*, *10*, 93–111, doi:10.1016/0377-0273(81)90057-3.

Parekh, P., M. J. Follows, and E. A. Boyle (2005), Decoupling of iron and phosphate in the global ocean, *Global Biogeochem. Cycles*, *19*, GB2020, doi:10.1029/2004GB002280.

Peters, J. L., R. W. Murray, J. W. Sparks, and D. S. Coleman (2000), Terrigenous matter and dispersed ash in sediment from the Caribbean Sea; results from Leg 165, *Proc. Ocean Drill. Program, Sci. Results*, *165*, 115–124.

Pyle, D. M. (1989), The thickness, volume and grain size of tephra fall deposits, *Bull. Volcanol.*, *51*, 1–15, doi:10.1007/BF01086757.

Rea, D. K. (1994), The paleoclimatic record provided by eolian deposition in the deep sea: The geologic history of wind, *Rev. Geophys.*, *32*, 159–195, doi:10.1029/93RG03257.

Rees, B., R. Detrick, and B. Coakley (1993), Seismic stratigraphy of the Hawaiian flexural moat, *Mem. Geol. Soc. Am.*, *105*, 189–205, doi:10.1130/0016-7606(1993)105<0189:SSOTHF>2.3.CO;2.

Rose, W. I. (1977), Scavenging of volcanic aerosol by ash: Atmospheric and volcanolgic implications, *Geology*, *5*, 621–624, doi:10.1130/0091-7613(1977)5<621:SOVABA>2.0.CO;2.

Rose, W. I., and A. J. Durant (2009), Fine ash content of explosive eruptions, *J. Volcanol. Geotherm. Res.*, *186*, 32–39, doi:10.1016/j.jvolgeores.2009.01.010.

Sarmiento, J. L. (1993), Atmospheric CO_2 stalled, *Nature*, *365*, 697–698, doi:10.1038/365697a0.

Schmincke, H. U., and M. Sumita (1998), Tephra event stratigraphy and emplacement of volcaniclastic sediments, Mogan and Fataga stratigraphic intervals, ODP leg 157. Part II: Origin and emplacement of volcaniclastic layers, *Weaver PPE*, 267–291.

Schroth, A. W., J. Crusius, E. R. Sholkovitz, and B. C. Bostick (2009), Iron solubility driven by speciation in dust sources to the ocean, *Nat. Geosci.*, *2*, 337–340, doi:10.1038/ngeo501.

Scudder, R. P., R. W. Murray, and T. Plank (2009), Dispersed ash in deeply buried sediment from the northwest Pacific Ocean: An example from the Izu–Bonin arc (ODP Site 1149), *Earth Planet. Sci. Lett.*, *284*, 639–648, doi:10.1016/j.epsl.2009.05.037.

Sedwick, P. N., E. R. Sholkovitz, and T. M. Church (2007), Impact of anthropogenic combustion emissions on the fractional solubility of aerosol iron: Evidence from the Sargasso Sea, *Geochem. Geophys. Geosyst.*, *8*, Q10Q06, doi:10.1029/2007GC001586.

Sigurdsson, H., B. Houghton, S. R. McNutt, H. Rymer, and J. Stix (Eds.) (2000), *Encyclopedia of Volcanoes*, Academic, San Diego, Calif.

Spirakis, C. S. (1991), Iron fertilization with volcanic ash, *Eos Trans. AGU*, *72*(47), 525, doi:10.1029/90EO00370.

Spokes, L. J., and T. D. Jickells (1996), Factors controlling the solubility of aerosol trace metals in the atmosphere and on mixing into seawater, *Aquat. Geochem.*, *1*, 355–374, doi:10.1007/BF00702739.

Straub, S. M., and H.-U. Schmincke (1998), Evaluating the tephra input into Pacific Ocean sediments: Distribution in space and time, *Geol. Rundsch.*, *87*, 461–476, doi:10.1007/s005310050222.

Textor, C., H. F. Graf, M. Herzog, J. M. Oberhuber, W. I. Rose, and G. G. J. Ernst (2006), Volcanic particle aggregation in explosive eruption columns. Part I: Parameterization of the microphysics of hydrometeors and ash, *J. Geothermal Res.*, *150*, 359–377, doi:10.1016/j.jvolgeores.2005.09.007.

Turner, S., N. Arnaud, J. Liu, N. Rogers, C. Hawkesworth, N. Harris, S. Kelley, P. van Calsteren, and W. Deng (1996), Post-collision, Shoshonitic Volcanism on the Tibetan Plateau: Implications for convective thinning of the lithosphere and the source of ocean island basalts, *J. Petrol.*, *37*, 45–71, doi:10.1093/petrology/37.1.45.

Turner, S. M., M. J. Harvey, C. S. Law, P. D. Nightingale, and P. S. Liss (2004), Iron-induced changes in oceanic sulfur biogeochemistry, *Geophys. Res. Lett.*, *31*, L14307, doi:10.1029/2004GL020296.

Viereck, L., M. Simon, and H.-U. Schmincke (1985), Primary composition, alteration, and origin of Cretaceous volcaniclastic rocks, East Mariana basin (site 585, leg 89), in *Initial Reports of DSDP*, edited by R. Moberly and S. Schlanger, pp. 529–553, U.S. Govt. Print. Off., Washington, D. C.

Watson, A. J. (1997), Volcanic Fe, CO_2, ocean productivity and climate, *Nature*, *385*, 587–588, doi:10.1038/385587b0.

Watson, A. J. (2001), Iron limitation in the oceans, in *The Biogeochemistry of Iron in Seawater*, edited by D. R. Turner and K. A. Hunter, pp. 9–39, John Wiley, West Sussex, U. K.

Watson, A. J., P. S. Liss, and R. A. Duce (1991), Design of a small scale iron enrichment experiment, *Limnol. Oceanogr.*, *36*, 1960–1965, doi:10.4319/lo.1991.36.8.1960.

Wells, M. L. (2003), The level of iron enrichment required to initiate diatom blooms in HNLC waters, *Mar. Chem.*, *82*, 101–114, doi:10.1016/S0304-4203(03)00055-0.

Wiesner, M. G., Y. Wang, and L. Zheng (1995), Fallout of volcanic ash to the deep South China Sea induced by the 1991 eruption of Mount Pinatubo (Philippines), *Geology*, *23*, 885–888, doi:10.1130/0091-7613(1995)023<0885:FOVATT>2.3.CO;2.

Winckler, G., R. F. Anderson, M. Q. Fleisher, D. McGee, and N. Mahowald (2008), Covariant glacial-interglacial dust fluxes in the equatorial Pacific and Antarctica, *Science*, *320*, 93–96, doi:10.1126/science.1150595.

Wolfe, C. J., M. K. McNutt, and R. S. Detrick (1994), The Marquesas archipelago apron: Seismic stratigraphy and implications for volcano growth, mass wasting, and crustal underplating, *J. Geophys. Res.*, *99*, 13,591–13,608, doi:10.1029/94JB00686.

Wu, J., R. Rember, and C. Cahill (2007), Dissolution of aerosol iron in the surface waters of the North Pacific and North Atlantic oceans as determined by a semicontinuous flow-through reactor method, *Global Biogeochem. Cycles*, *21*, GB4010, doi:10.1029/2006GB002851.

Zhuang, G., Z. Yi, R. A. Duce, and P. R. Brown (1992), Chemistry of iron in marine aerosols, *Global Biogeochem. Cycles*, *6*, 161–173, doi:10.1029/92GB00756.

A. Auer, Department of Geology, University of Otago, PO Box 56, Dunedin 9054, New Zealand.

P. L. Croot, Marine Biogeochemistry, Plymouth Marine Laboratory, Prospect Place, Plymouth PL1 3DH, UK.

P. Delmelle, Environment Department, University of York, Heslington, York YO10 5D, UK.

S. Duggen, A. P. Møller Skolen, Upper Secondary School and Sixth Form College of the Danish National Minority in Northern Germany, Fjordallee 1, Schleswig D-24837, Germany.

D. Garbe-Schönberg, Institute of Geosciences, Universtity of Kiel, Olshausenstrasse 40, Kiel D-24118, Germany.

H. Dietze and N. Olgun, Marine Biogeochemistry Division, Leibniz-Institute of Marine Sciences, IFM-GEOMAR, Düsternbrooker Weg 20, Kiel D-24105, Germany. (nolgun@ifm-geomar.de)

N. Óskarsson, Institute of Earth Sciences, University of Iceland, Askja, Sturlugata 7, Reykjavík 101, Iceland.

U. Schacht, CO2CRC, Australian School of Petroleum, University of Adelaide, Gate 6, Frome Road, Adelaide SA 5005, Australia.

C. Siebe, Departamento de Vulcanología, Instituto de Geofísica, Universidad Nacional Autónoma de México, Ciudad Universitaria, 04510 Coyoacán, Mexico.